ITTC Quality System Manual
Recommended Procedures and Guidelines

Procedure

Avoiding Self-Repeating Effect in Time-Domain Numerical Simulation of Ship Motions

7.5	Process Control
7.5-02	Testing and Extrapolation Methods
7.5-02-01	General
7.5-02-01-09	Avoiding Self-Repeating Effect in Time-Domain Numerical Simulation of Ship Motions

Updated / Edited by	Approved
Stability in Waves Committee of the 30th ITTC	30th ITTC 2024
Date: 08/2024	Date: 09/2024

Table of Contents

Avoiding Self-Repeating Effect in Time-Domain Numerical Simulation of Ship Motions

1. PURPOSE OF PROCEDURE

The purpose of this procedure is to formulate a process for verification of absence of self-repeating effect and statistical validity of irregular waves in a numerical simulation. The procedure provides specific guidelines to check the self-repeating effect for the direct stability assessment as defined in section 3.3.2.1 of Interim Guidelines on The Second Generation Intact Stability Criteria MSC.1/Circ. 1627 (IMO 2020) and in section 3.3.2.1 of Explanatory Notes to the Interim Guidelines on The Second Generation Intact Stability Criteria MSC.1/Circ. 1652 (IMO 2023), cited further for brevity just as the Interim Guidelines and Explanatory Notes, respectively.

Meanwhile, avoiding self-repeating effect is important to evaluate accurately the hydrodynamic performance in irregular waves, specifically for adequate uncertainty quantification. Therefore, this recommended procedure can also be useful for seakeeping and ocean engineering problems where account for randomness of waves is required.

2. SIMULATION OF IRREGULAR WAVES

2.1 Wave spectrum

The motion characteristics of ships can be estimated by employing the proper spectrum model of ocean waves. The spectrum should be able to describe the specific characteristics of certain sea site where subject ships would sail.

The two parameters spectrum is quite common for describing a wide range of site-specific wave condition. The spectral density, S_W, can be written with general form, as follows:

$$S_W(\omega) = \frac{A}{4} H_S^2 \frac{\tilde{\omega}^4}{\omega^5} \exp\left(-A\left(\frac{\tilde{\omega}}{\omega}\right)^4\right) \tag{1}$$

where H_S is significant wave height, ω is circular frequency, while A and $\tilde{\omega}$ are parameters defined in Table 1.

The Pierson-Moskowitz (P-M), Bretschneider (1959), ISSC and ITTC spectra are defined with these parameters, and their relation can be found in Table 1 (Chakrabarti 1987).

Table 1 Coefficient and relationship of two parameter wave spectrum

Model	A	$\tilde{\omega}$	$\tilde{\omega}/\omega_0$	$\tilde{\omega}/\overline{\omega}$	$\tilde{\omega}/\omega_Z$
P-M	5/4	ω_0	1.0	0.772	0.710
Bretschneider	0.675	ω_S	1.167	0.9	0.829
ISSC	0.4427	$\overline{\omega}$	1.296	1.0	0.921
ITTC	5/4	ω_0	1.0	0.772	0.710

where

ω_0 is peak frequency
ω_S is significant frequency
$\overline{\omega}$ is mean frequency
ω_Z is mean zero-crossing frequency

Other types of spectrum models are available with different energy density distributions with respect to the wave frequencies (e.g. Chakrabarti 1987; Ochi 1998; ITTC 2021).

2.2 Generation of wave time series for long-crested sea

Linear superposition of regular wave components is commonly applied to construct time series of irregular wave elevations, ζ_W:

$$\zeta_W(t) = \sum_{i=1}^{N} A_i \cos(\omega_i t + \varphi_i) \quad (2)$$

t is time, ω_i is a frequency of i-th wave component, φ_i is phase shift of i-th component, it is uniformly distributed in [0, 2π). The wave amplitude of i-th component, A_i, is determined from the segment of wave spectrum and selected wave frequency.

$$A_i = \sqrt{2S_W(\omega_i)\Delta\omega_i} \quad (3)$$

The i-th frequency increment $\Delta\omega_i$ is a result of either equal or unequal discretization between the lowest, ω_{min}, and the highest, ω_{max}, cut-off frequencies.

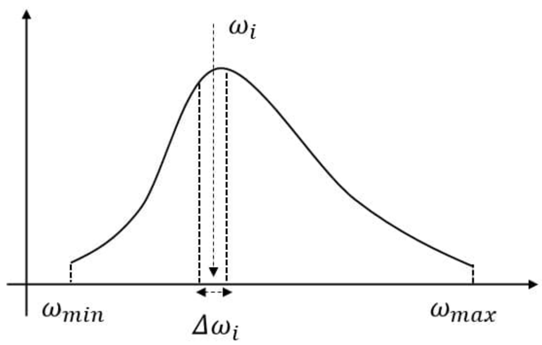

Figure 1: Discretization of wave spectrum

No recommended procedure for determining the upper and lower cut-off frequencies is available from ITTC Guideline 7.5-02 07-01.1, however the truncation should be minimized in order to reduce the loss of total wave energy.

2.3 Generation of wave time series for short-crested sea

Short-crested seas can be simulated in a similar way to long-crested seas, once the directional probability distribution is taken into account.

$$\zeta_W(t) = \sum_{i=1}^{N} A_{si} \cos(\omega_i t + \varphi_i) \quad (4)$$

where

$$A_{si} = \sqrt{2S_w(\omega_i)D(\mu_i)\Delta\omega_i\Delta\mu_i} \quad (5)$$

The directional probability distribution function $D(\mu_i)$ for discretized heading angle μ_i has various form. The cosine spreading function is commonly employed for wind waves (DNV 2021).

$$D(\mu_i) = \frac{\Gamma(1+n/2)}{\sqrt{\pi}\Gamma(1/2+n/2)}\cos^2(\mu_i - \mu_0) \quad (6)$$

where μ_0 is an angle of general direction of wave propagation and

$$|\mu_i - \mu_0| \le \pi/2 \quad (7)$$

The various type of the spreading functions can be found in ITTC Guideline 7.5-02 07-01.1, ITTC (2017).

Short-crested wave model provides a more realistic description of the real ocean waves. However, it requires more computational resources since a set of irregular waves from different directions needs to be summarized.

3. EXAMINATION OF SELF-REPEATING EFFECT USING AUTOCORRELATION FUNCTION

The self-repeating effect of wave model is induced by a numerical error of spectral discretization into a finite number of segments. The detailed explanation on origin of this numerical error, leading to the self-repeating effect can be found in Appendix A.

Presence or absence of the self-repeating effect can be verified with an autocorrelation or autocovariance function. These functions indicate covariance or correlation of a single value of a stochastic process random with itself after some time, commonly referenced as time-lag. This autocorrelation should converge to zero, as time lag gets longer, if no physical reason exists for the dependency to last.

The autocovariance of irregular waves can be calculated from the wave spectrum, as described in section 3.3.2.1 of the Appendix 4 to the Explanatory Notes, IMO (2023), (also Belenky 2011)

$$R(\tau_j) = \int_0^\infty S_w(\omega)\cos(\omega\tau_j)\,d\omega \qquad (8)$$

where R is the autocovariance function of wave elevations and τ is the time lag. The autocovariance function of zero lag equals to variance of the wave elevations. The autocorrelation function r is the autocovariance function, normalized by its first term, i.e. by variance:

$$r(\tau_j) = R(\tau_j)/R(0) \qquad (9)$$

For the purposes of detection of the self-repeating effect in wave model, the autocovariance function needs to be calculated from the spectrum with the same frequency discretization, as being planned for wave elevation reconstruction for ship motion simulations. The numerical integration in equation (8) has to be carried out with rectangles, as this method is applied in in equation (2):

$$R(\tau_j) = \sum_{i=1}^{N} S_W(\omega_i)\cos(\omega_i\tau_j) \qquad (10)$$

If the self-repeating effect does not present in the wave-elevation time series of duration $T = \tau_{max}$ the autocorrelation function is "clean", and does not have any increase after initial decay in Figure 2.

If the self-repeating effect is present, its appearance may be different, depending on the frequency discretization. If the frequencies distributed uniformly, i.e. frequency increment $\Delta\omega_i$ is constant, the presence of self-repeating effect is observed as "spikes" in the autocorrelation plot in Figure 3.

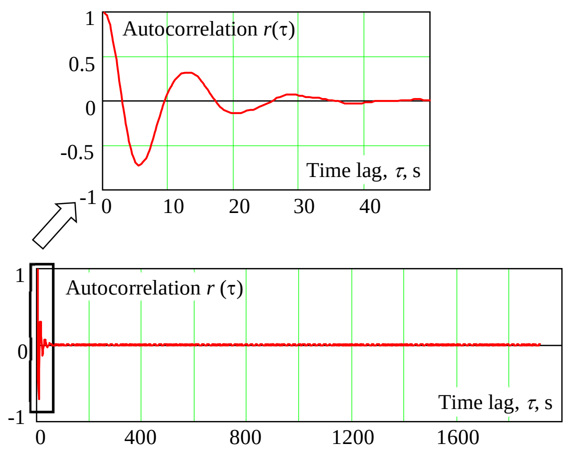

Figure 2: Autocorrelation function in absence of self-repeating effect (MSC.1/Circ. 1652, IMO 2023)

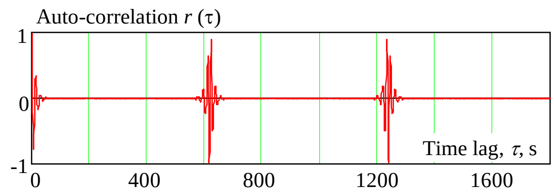

Figure 3: Autocorrelation function showing presence of self-repeating effect for uniformed discretization or constant frequency increment

If a non-uniformed frequency distribution is applied (i.e. the frequency increment $\Delta\omega_i$ varies), the presence of the self-repeating effect is observed as a series of increasing oscillations in Figure 4.

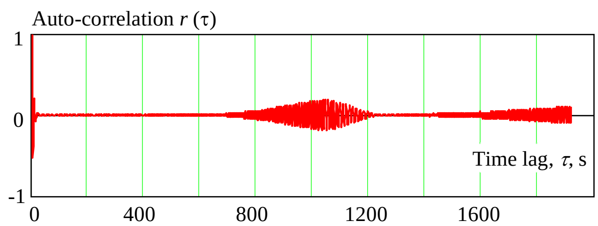

Figure 4: Autocorrelation function showing presence of self-repeating effect for non-uniformed discretization or variable frequency increment

Due to its nature (Appendix A), the self-repeating effect will reveal itself eventually. The practical question is what duration of wave elevation time series is still valid for a give discretization of frequencies. Answer to this question in case of uniformed frequency distribution is evident: beginning of the “spike” of the autocorrelation function limits valid duration of a record.

For the case of non-uniformed frequency distribution, an envelope of autocorrelation function is be useful to find when the of signal starts to increase. The envelope is constructed by connecting absolute values of the peaks of autocorrelation function. Paragraph 3.7.18 of Annex 4 to the Explanatory Notes suggests using the value of autocorrelation of 0.05 to determine limits valid duration of a record in Figure 5.

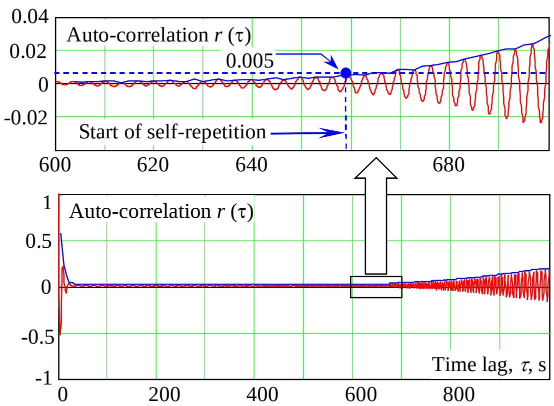

Figure 5: Determination of inception of self-repeating effect (MSC.1/Circ. 1652, IMO 2023)

The self-repeating effect is sensitive to encounter frequencies. If the ship advances with certain forward speed U, the encounter wave frequencies should be applied instead of true wave frequencies. The i-th component of encounter frequency, ω_{ei}, can be calculated from original wave frequency with the wave number, k_i, and relative heading angle, μ.

$$\omega_{ei} = \omega_i - k_i U \cos\mu \tag{11}$$

where:

$$k_i = \omega_i^2 / g \tag{21}$$

where g is the gravity acceleration.

Even though increasing the number of wave frequencies is appropriate way avoiding self-repeating effect, it is practically not efficient for time-domain computation. The computational cost for many wave component may be substantial. Many relatively short records may be more computationally efficient compared to a single long record.

4. LIST OF SYMBOLS

A	Spectral parameter	
A_i	Amplitude of i-th component for long-crested waves,	[m]
A_{si}	Amplitude of i-th component for short-crested waves,	[m
D	Spreading function for short-crested waves	
g	Gravity acceleration,	[m/s^2]
H_s	Significant wave height,	[m]
k_i	Wave number, corresponding to i-th component,	[m^{-1}]
R	Autocovariance function,	[m^2]
r	Autocorrelation function	
S_W	Spectral density,	[m^2·s]
T	Duration of simulation,	[s]
T_m	Modal period,	[s]
t	Time,	[s]
U	Forward speed,	[m/s]
μ	Relative heading angle	
μ_i	Heading angle for i-th component	
μ_0	Angle of general direction of wave propagation (for long-crested waves)	
τ	Time lag of autocovariance or autocorrelation function,	[s]
$\Delta\omega_i$	Frequency increment,	[s^{-1}]
φ_i	Phase shift of i-th component	
ζ_W	Wave elevation,	[m]
$\tilde{\omega}$	Spectral parameter,	[s^{-1}]
ω_{ei}	Encounter frequency of i-th component,	[s^{-1}]

ω_i	Frequency of *i*-th component,	[s^{-1}]
ω_{min}	Low cut-off frequency,	[s^{-1}]
ω_{max}	High cut-off frequency,	[s^{-1}]
ω_S	Significant frequency,	[s^{-1}]
ω_Z	Mean zero-crossing frequency	[s^{-1}]
ω_0	Peak frequency,	[s^{-1}]

5. REFERENCES

Belenky, V. (2011) "On Self-Repeating Effect in Reconstruction of Irregular Waves," Chapter 33 of *Contemporary Ideas on Ship Stability*, Neves, M. A. S., Belenky, V., de Kat, J. O., Spyrou, K., and Umeda, N., eds., Springer, ISBN 978-94-007-1481-6, pp. 589-598.

Bretschneider, C. L. (1959) "Wave Variability and Wave Spectra for Wind-Generated Gravity Waves," U. S. Army Beach Erosion Board, Technical Memorandum 118, Washington, DC, USA.

Chakrabarti, S. K. (1987) *Hydrodynamics of Offshore Structures*, WIT Press, Southampton, UK.

DNV (2021) "Environmental Conditions and Environmental Loads," Recommended Practice, DNV-RP-C205, DNV, Oslo, Norway.

IMO MSC.1/Circ.1627, "Interim guidelines on the second-generation intact stability criteria", London, UK, December 2020.

IMO MSC. 1/Circ.1652, "Explanatory notes for interim guidelines on the second-generation intact stability criteria," London, UK, April 2023.

ITTC (2017) "Laboratory Modelling of Multidirectional Irregular Wave Spectra," ITTC Guideline, 7.5-02 07-01.1 Revision 1, International Towing Tank Conference.

ITTC (2021) "Laboratory Modelling of Waves," ITTC Guideline, 7.5-02 07-01.2, Revision 1, International Towing Tank Conference.

Ochi, M. K. (1998) Ocean Waves, Cambridge University Press, Cambridge, UK.

Tsoumpelis, D. & K. J. Spyrou (2023) "Identification of Recurring Patterns and Repetitions in Time-series, with Application to Pseudo-stochastic Ship Rolling," *Ocean Eng.*, Special Issue on Extreme Stochastic Dynamics Ships, Vol. 271, 113717.

Umeda, N., Y. Maruyama, S. Okamoto, A. Oka, S. Masamoto & A. Matsuda (2023) Filling Gaps in Direct Stability Assessment Procedures, *Proc. 19th Int'l Ship Stability Workshop*, Istanbul, Turkey, pp. 193-200.

Appendix A. ON UNIFORM FREQUENCY DISCRETIZATION OF SPECTRAL DENSITY

A.1. Formulation of the problem

The wave elevation at a fixed point in space, expressed with equation (2), uses inverse Fourier transformation of the spectral density and is commonly referenced as Longuett-Higgins model.

The equation (2) is probabilistically valid on a limited time interval. The autocorrelation function begins to increase outside of this interval, and the model demonstrates dependence, where the real stochastic process should not have it. This limitation of validity is the essence of self-repeating effect in model (2) leading to partial self-repetition of the constructed wave elevation time series (Belenky 2011; Tsoumpelis and Spyrou 2023, Umeda et al. 2023).

For the uniform frequency discretization the period of validity was found to be short of $T = 2\pi/\Delta\omega$; however, no formal proof was given.

An attempt to give it a more formal consideration is made here.

An example with Bretschneider (1959) spectrum illustrates further considerations in Figure A1. A discretization with 20 frequencies is applied within the interval $\omega \in [0.272; 1.068]$ with $\Delta\omega = 0.042$ rad/s. The discretized power spectrum is in Figure A2.

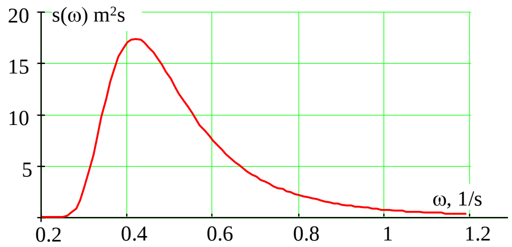

Figure A1: Spectral density of wave elevations for significant wave height H_s = 15 m and modal period T_m = 15 s

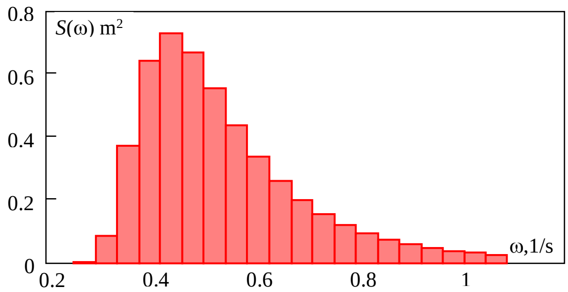

Figure A2: Discretized power spectrum with 20 frequencies $\omega \in [0.272; 1.068]$ with $\Delta\omega = 0.042$ rad/s.

A.2. Integrand of Autocorrelation Function

Autocovariance function for detection of the self-repeating effect is expressed in equation (8), while the autocorrelation function is the autocovariance, normalized by the variance, i.e. the autocovariance at τ = 0, equation (9). The autocorrelation function computed for 200 seconds is in Figure A3.

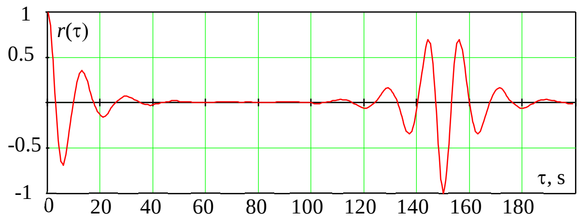

Figure A3: Autocorrelation function computed with 20 Frequencies $\omega \in [0.272; 1.068]$ with $\Delta\omega = 0.042$ rad/s.

The self-repeating effect starts somewhere around 110th second, while its "period" is $T = 2\pi/\Delta\omega \approx 150$ s. This value corresponds to the largest negative peak of the autocorrelation function. It is in the "middle" of the self-repeating effect.

The reason for the self-repeating effect is rooted in an oscillatory nature of the integrand in equation (10). Its frequency increases with the increased time lag τ in Figure A4.

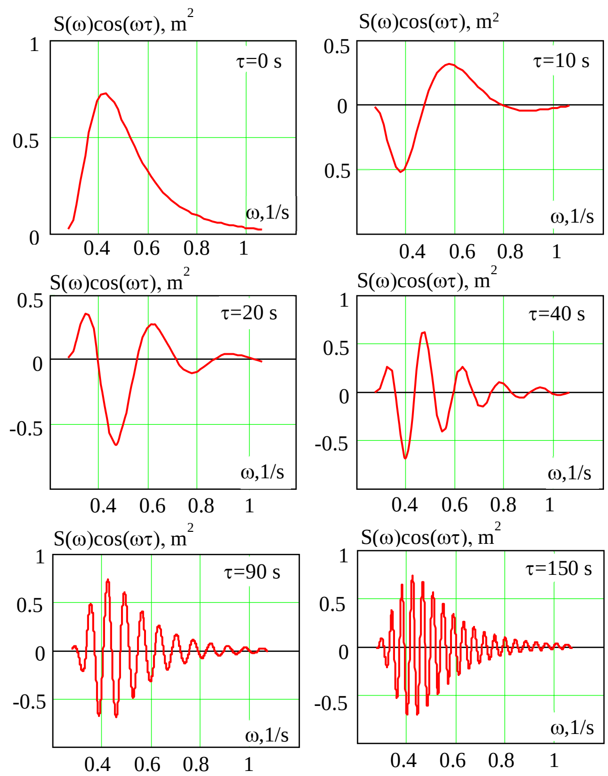

Figure A4: Oscillatory behaviour of the integrand $s(\omega_i)\cos(\omega_i\tau)$ with increase of the time lag

Numerical accuracy of integration with rectangular method with the constant $\Delta\omega$ of the integrand $s(\omega_i)\cos(\omega_i\tau)$ depends on time lag. When the time lag is small, $\Delta\omega = 0.042$ rad/s is sufficient in, see Figure A5. That is why values of auto-correlation function are accurate for these small lags. The period of oscillation of the integrand in frequency domain depends only on the time lag:

$$\Omega_I = 2\pi/\tau \tag{A1}$$

The rectangular discretization of the integrand computed for 70 seconds is shown in Figure A6. The accuracy is already decreased. The rectangular discretization misrepresents some of the laps. However, no laps are missed, because the period of oscillation at 70 seconds larger than two frequency increments. At least two frequency increments occur per period of the integrand. The low accuracy does not have much influence on the final result here, as the value of autocorrelation function is quite close to zero, $r(70) = 0.004355$. The accuracy of the calculations is acceptable, while the positive values of the integrand balance its negative values.

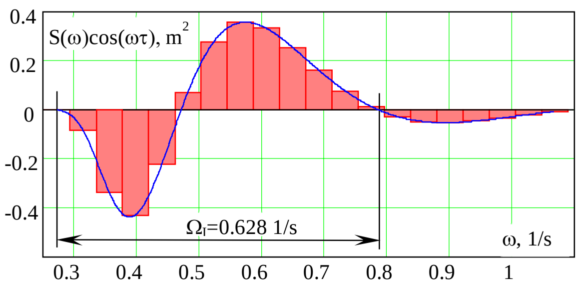

Figure A5: Rectangular numerical integration of $s(\omega_i)\cos(\omega_i\tau)$ with $\Delta\omega = 0.042$ rad/s for $\tau = 10$ s, period of the oscillation 0.628 rad/s

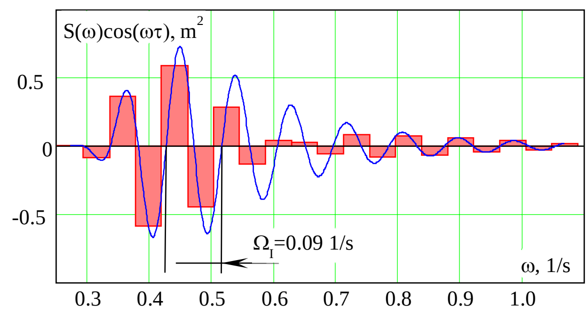

Figure A6 Rectangular numerical Integration of $S(\omega_i)\cos(\omega_i\tau)$ with $\Delta\omega = 0.042$ rad/s for $\tau = 70$ s, period of the oscillation 0.09 rad/s

For the time lag $\tau = 75$ s (the half of the expected time to peak of the self-repeating effect $T = 2\pi/\Delta\omega$), the period of oscillations of the integrand is exactly twice of the frequency increment: $\Omega_I = 0.084$, the value of the autocorrelation function by equation (10) is exactly zero in Figure A7. The values of the integrand are computed at the point, when the cosine function crosses the axis.

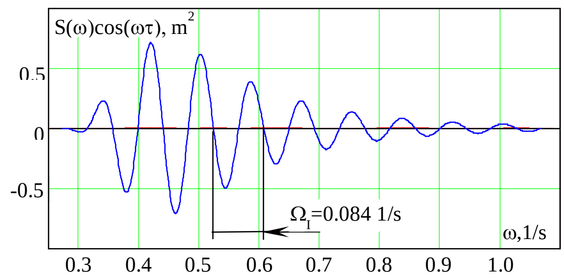

Figure A7: Rectangular numerical integration of $S(\omega_i)\cos(\omega_i\tau)$ with $\Delta\omega = 0.042$ rad/s for $\tau = 75$ s, period of the oscillation 0.084 rad/s

The time lag $\tau = 90$ s is shown in Figure A8, where the period of oscillation of the integrand is 0.07. Some laps are missed. However, the value of the autocorrelation function is still very small, $r(70) = 0.00315$. Even these two missed laps did not cause deterioration of the accuracy.

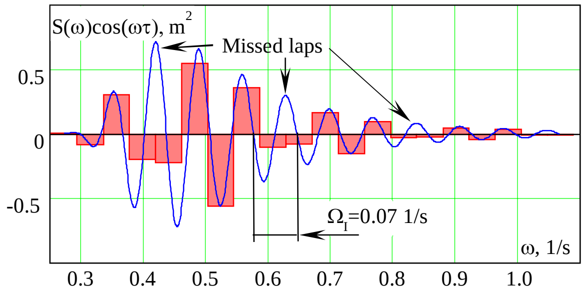

Figure A8: Rectangular numerical integration of $S(\omega_i)\cos(\omega_i\tau)$ with $\Delta\omega = 0.042$ rad/s for τ = 90 s, period of the oscillation 0.07 rad/s

The time lag τ = 110 s is shown in Figure A9, where the self-repeating effect is fully developed. The period of oscillation of the integrand is 0.063, twelve laps out of 29 (number of laps can be calculated, as $2(\omega_N - \omega_1)/\Omega_I$) is missed. The value of the autocorrelation function exceeds 1.0 %, r(110) = 0.028. These missed laps seem to not to influence the accuracy too much.

Finally, at the self-repeating "peak value" $\tau = 2\pi/\Delta\omega \approx 150$ s, half of the laps are missing in Figure A10. The value of autocorrelation function is r(150) = -1.0. The value of $2\pi/\Delta\omega$ is the time, when numerical inaccuracy of formula (10) becomes the largest.

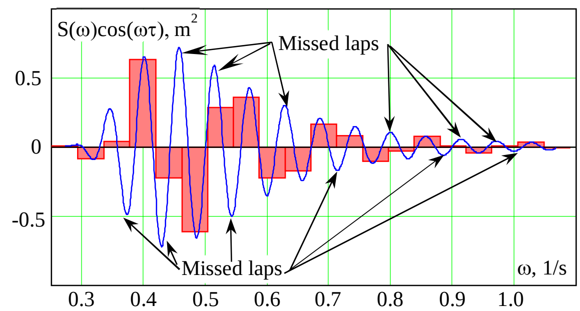

Figure A9: Rectangular numerical integration of $S(\omega_i)\cos(\omega_i\tau)$ with $\Delta\omega = 0.042$ rad/s for τ = 110 s, period of the oscillation 0.057 rad/s

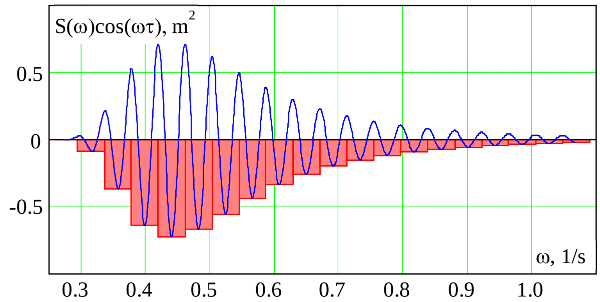

Figure A10: Rectangular numerical Integration of $S(\omega_i)\cos(\omega_i\tau)$ with $\Delta\omega = 0.042$ rad/s for τ = 150 s, period of the oscillation 0.042 rad/s

A.3. Integrand of Inverse Fourier Transform

The interpretation of the meaning of $2\pi/\Delta\omega$ performed with an integrand of autocorrelation function (10) can be formally extended the model of stochastic process (2). Equation (10) is a true representation of autocorrelation function of process (2) if the same frequency discretization is used. However, a practitioner may benefit from numerical demonstration that the observed behavior of the integrand of the autocorrelation function (10) leads to the similar behavior of the integrand of the process itself.

First, expand the cosine function in the integrand of the equation (2)

$$\zeta_W(t) = \sum_{i=1}^{N}[A_i\cos(\omega_i t)\cos(\varphi_i) - A_i\sin(\omega_i t)\sin(\varphi_i)] \tag{A2}$$

Both cosine and sine component of the integrand contain random terms: $\cos(\varphi_i)$ and $\sin(\varphi_i)$, as well as deterministic terms: $A_i\cos(\omega_i t)$ and $A_i\sin(\omega_i t)$. Figure A11 illustrates separately random and deterministic term of each component.

The deterministic part can be considered in Figure A11, as some sort of an envelope for the cosine of sine component of the integrand part. Thus, if the frequency discretization is sufficient, for accurate representation of the deterministic part, it should be good enough for the entire integrand in Figure A12. Blue line identifies the deterministic part of the integrand, computed with higher frequency resolution, while red bars present the considered discretization with 20 frequencies.

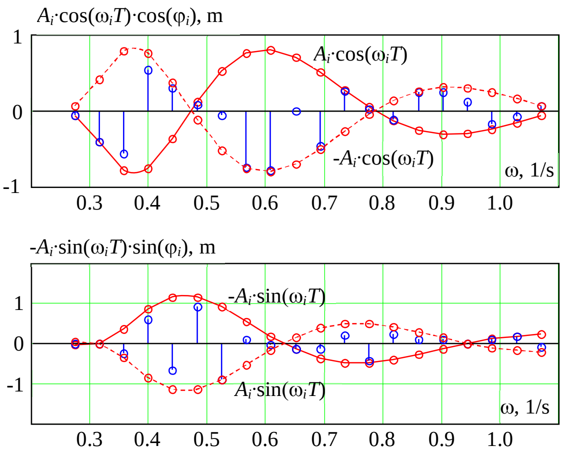

Figure A11: Structure of the integrand of the inverse Fourier transformation with $\Delta\omega = 0.042$ rad/s for τ = 10 s

Figure A13 depicts how the sine and the cosine of the integrand look for the time instant of 110 seconds, where the self-repeating effect starts to manifest itself. The blue line is the deterministic part of the integrand, computed with high-resolution frequency set. The considered 20-frequencies discretization make poor representation of the integrand. The picture is somewhat similar to the integrand of the autocorrelation function in Figure A8.

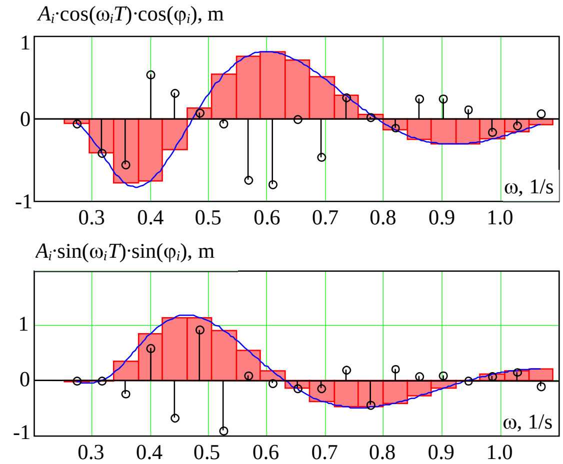

Figure A12: Rectangular numerical integration for the inverse Fourier transformation with $\Delta\omega = 0.042$ rad/s for τ = 10 s

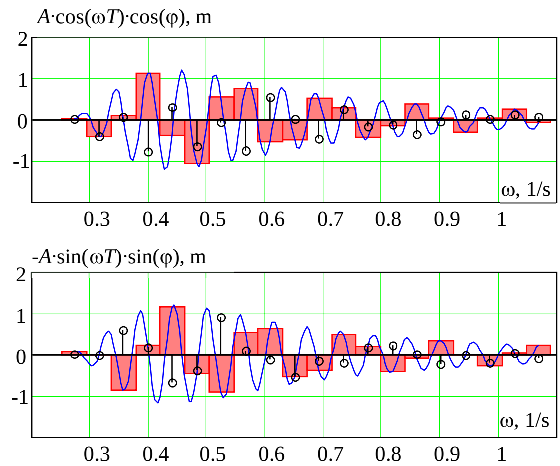

Figure A13: Rectangular numerical Integration for the inverse Fourier transformation with $\Delta\omega = 0.042$ rad/s for τ = 110 s

The behavior of the integrands of autocorrelation function (10) and the inverse Fourier transformation (2) are similar in the example. The reason for self-repeating effect in equation (2) is deteriorating of the accuracy of numerical integration, as it could be observed in autocorrelation function (10).